Received: 3 January 2020 | Revised: 26 March 2020 | Accepted: 14 April 2020

DOI: 10.1002/hbm.25023

RESEARCH ARTICLE

WILEY

Grab-AD: Generalizability and reproducibility of altered brain activity and diagnostic classification in Alzheimer's Disease

Dan Jin[1,2] | Pan Wang[3] | Andrew Zalesky[4,5] | Bing Liu[1,2,6] | Chengyuan Song[7] | Dawei Wang[8] | Kaibin Xu[1] | Hongwei Yang[9] | Zengqiang Zhang[10] | Hongxiang Yao[11] | Bo Zhou[12] | Tong Han[13] | Nianming Zuo[1,2] | Ying Han[14,15,16,17] | Jie Lu[9] | Qing Wang[8] | Chunshui Yu[18] | Xinqing Zhang[14] | Xi Zhang[12] | Tianzi Jiang[1,2,6] | Yuying Zhou[3] | Yong Liu[1,2,6]

[1]Brainnetome Center & National Laboratory of Pattern Recognition, Institute of Automation, Chinese Academy of Sciences, Beijing, China

[2]School of Artificial Intelligence, University of Chinese Academy of Sciences, Beijing, China

[3]Department of Neurology, Tianjin Huanhu Hospital, Tianjin University, Tianjin, China

[4]Melbourne Neuropsychiatry Centre, Department of Psychiatry, University of Melbourne and Melbourne Health, Melbourne, Victoria, Australia

[5]Department of Biomedical Engineering, University of Melbourne, Melbourne, Victoria, Australia

[6]Center for Excellence in Brain Science and Intelligence Technology, Institute of Automation, Chinese Academy of Sciences, Beijing, China

[7]Department of Neurology, Qilu Hospital of Shandong University, Ji'nan, China

[8]Department of Radiology, Qilu Hospital of Shandong University, Ji'nan, China

[9]Department of Radiology, Xuanwu Hospital of Capital Medical University, Beijing, China

[10]Branch of Chinese PLA General Hospital, Sanya, China

[11]Department of Radiology, the Second Medical Centre, National Clinical Research Centre for Geriatric Diseases, Chinese PLA General Hospital, Beijing, China

[12]Department of Neurology, the Second Medical Centre, National Clinical Research Centre for Geriatric Diseases, Chinese PLA General Hospital, Beijing, China

[13]Department of Radiology, Tianjin Huanhu Hospital, Tianjin, China

[14]Department of Neurology, Xuanwu Hospital of Capital Medical University, Beijing, China

[15]Beijing Institute of Geriatrics, Beijing, China

[16]National Clinical Research Center for Geriatric Disorders, Beijing, China

[17]Center of Alzheimer's Disease, Beijing Institute for Brain Disorders, Beijing, China

[18]Department of Radiology, Tianjin Medical University General Hospital, Tianjin, China

Correspondence
Yong Liu, Brainnetome Center, Institute of Automation, Chinese Academy of Sciences, Beijing 100190, China.
Email: yliu@nlpr.ia.ac.cn

Yuying Zhou, Department of Neurology, Tianjin Huanhu Hospital, Tianjin, 300350 China.
Email: qiying789@sina.cn

Abstract

Alzheimer's disease (AD) is associated with disruptions in brain activity and networks. However, there is substantial inconsistency among studies that have investigated functional brain alterations in AD; such contradictions have hindered efforts to elucidate the core disease mechanisms. In this study, we aim to comprehensively characterize AD-associated functional brain alterations using one of the world's largest resting-state functional MRI (fMRI) biobank for the disorder. The biobank includes

Dan Jin and Pan Wang contributed equally to this work.

This is an open access article under the terms of the Creative Commons Attribution-NonCommercial License, which permits use, distribution and reproduction in any medium, provided the original work is properly cited and is not used for commercial purposes.
© 2020 The Authors. *Human Brain Mapping* published by Wiley Periodicals LLC

Funding information
Beijing Municipal Sciences & Technology Commission, Grant/Award Number: Z171100000117001; National Key Research and Development Program of China, Grant/Award Numbers: 2016YFC1305904, 2018YFC2001700; National Natural Science Foundation of China, Grant/Award Numbers: 81871438, 81901101, 61633018, 81571062, 81701781; Strategic Priority Research Program (B) of the Chinese Academy of Sciences, Grant/Award Number: XDB32020200

fMRI data from six neuroimaging centers, with a total of 252 AD patients, 221 mild cognitive impairment (MCI) patients and 215 healthy comparison individuals. Meta-analytic techniques were used to unveil reliable differences in brain function among the three groups. Relative to the healthy comparison group, AD was associated with significantly reduced functional connectivity and local activity in the default-mode network, basal ganglia and cingulate gyrus, along with increased connectivity or local activity in the prefrontal lobe and hippocampus ($p < .05$, Bonferroni corrected). Moreover, these functional alterations were significantly correlated with the degree of cognitive impairment (AD and MCI groups) and amyloid-β burden. Machine learning models were trained to recognize key fMRI features to predict individual diagnostic status and clinical score. Leave-one-site-out cross-validation established that diagnostic status (mean area under the receiver operating characteristic curve: 0.85) and clinical score (mean correlation coefficient between predicted and actual Mini-Mental State Examination scores: 0.56, $p < .0001$) could be predicted with high accuracy. Collectively, our findings highlight the potential for a reproducible and generalizable functional brain imaging biomarker to aid the early diagnosis of AD and track its progression.

KEYWORDS
activity, Alzheimer's disease, functional connectivity, multicenter, resting-state fMRI

1 | INTRODUCTION

Alzheimer's disease (AD), one of the most common subtypes of dementia, is a neurodegenerative disorder characterized by memory deficits, cognitive impairment and executive dysfunction (Braak & Braak, 1991; Scheltens et al., 2016). Mild cognitive impairment (MCI) is suggested to be an intermediate state between normal aging and dementia (Academy of Cognitive Disorders of China, et al., 2020; Gauthier, et al., 2006). Network neuroscience can be applied to understand the pathogenesis and putative neural mechanisms that underlie these abnormalities (Bullmore & Sporns, 2012; Filippi et al., 2017; Fornito & Bullmore, 2015).

Functional magnetic resonance imaging (fMRI) studies in AD indicate that the disease is associated with widespread disruptions in brain functional networks, suggesting that AD may be conceptualized as a disconnection syndrome (Delbeuck, Collette, & Van der Linden, 2007; Delbeuck, Van der Linden, & Collette, 2003; Dennis & Thompson, 2014; Eyler et al., 2019; Liu et al., 2014; Wang et al., 2007, 2013). Despite an abundance of evidence, the reported findings are somewhat inconsistent among different studies, and the core regions associated with the pathogenesis of AD remain controversial. For example, Table S1 provides an overview of the disparity in findings among AD studies of whole-brain functional connectivity inferred from resting-state fMRI (Bai et al., 2011; Liang et al., 2014; Liu et al., 2012; Liu et al., 2014; Sanz-Arigita et al., 2010; Wang et al., 2007, 2013; Zhan et al., 2016; Zhou et al., 2015). One important reason for this inconsistency may be the heterogeneity inherent to small sample sizes and different analyses or acquisition protocols, resulting in poor reproducibility (Button et al., 2013; Davatzikos, 2019). In order to overcome this limitation, meta-analyses can be performed to combine findings across multiple independent studies (Jacobs, Radua, Luckmann, & Sack, 2013; Li et al., 2015; Pan et al., 2017; Xia, et al., 2019). However, meta-analytic approaches cannot address the heterogeneity associated with variation in data processing pipelines and differences in methodological and statistical approaches. For example, anatomical labels may vary between each study comprising a meta-analysis, resulting in mismatches in regional effects (Costafreda, 2009; Eickhoff, Yeo, & Genon, 2018). Another potential reason for the inconsistency of findings across previous studies is the use of relatively coarse-grained brain parcellation schemes to map whole-brain functional networks; these schemes do not adequately characterize regional boundaries in functional connectivity.

The key aim of the present study is to assess the robustness of aberrant patterns of brain activity and functional dysconnectivity in AD, and to focus on the reproducibility and generalizability of AD-related functional brain alterations as an imaging biomarker for early diagnosis and to track the progression of AD. For this purpose, we utilized a large AD biobank of resting-state fMRI (rs-fMRI) scans comprising 668 individuals acquired from six different MRI scanners to systematically investigate functional brain alterations in AD using four popularly used rs-fMRI measures. The fMRI data were processed consistently and analyzed using the same methodology for each scanner site. Meta-analyses were performed to combine data from the individual scanners and test for differences in functional connectivity and activity among AD patients, MCI patients and a healthy comparison group (Figure 1). We hypothesized that (a) individual variation in the extent of functional connectivity disruptions would be associated with cognitive impairments and

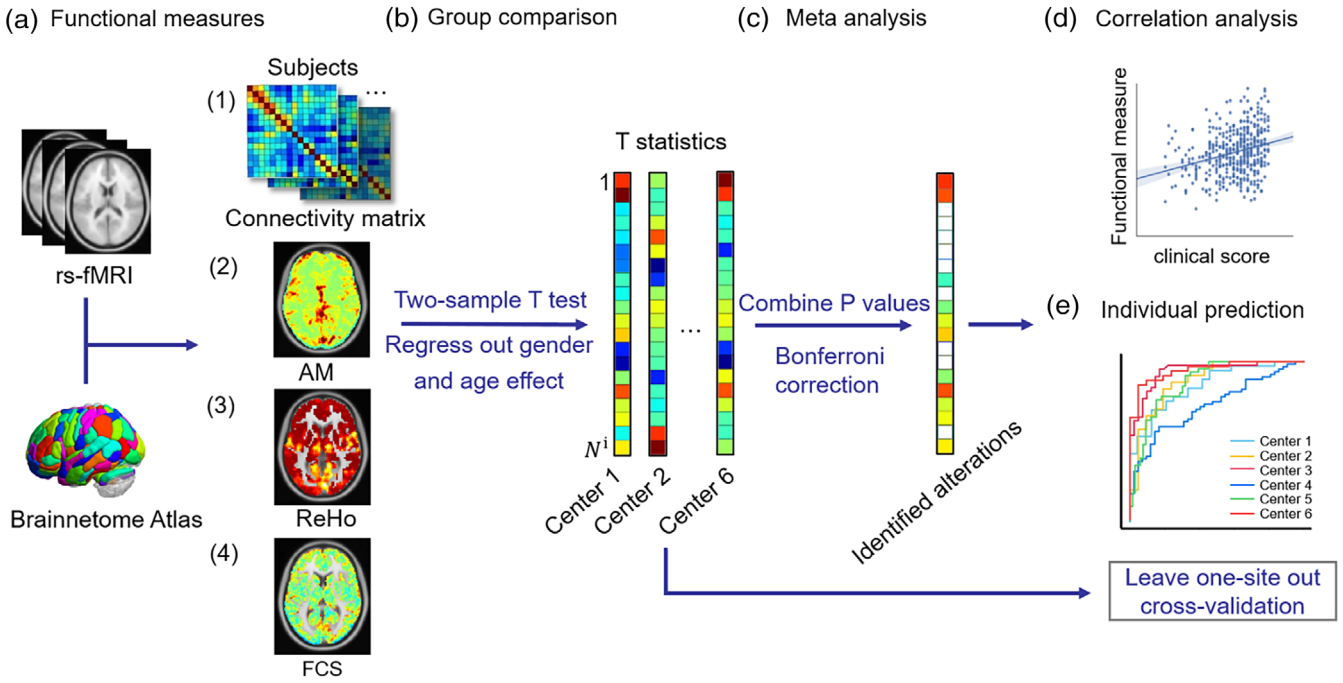

FIGURE 1 Schematic of the data analysis pipeline. (a) Functional measures (AM, ReHo, FCS) and the connectivity matrix are calculated based on Brainnetome Atlas. (b) A two-sample *t* test was performed to obtain the *p* value for each functional measure and connectivity in each center after controlling for age and gender effects. (c) The meta-analysis was applied to integrate results from six centers, and the significantly altered regions were identified after multiple comparison correction. (d) Then, the correlation analysis was performed to evaluate the relationship between functional measures and the clinical scores. (e) Finally, leave-one-site-out cross-validation was performed. AM, the amplitude of local brain activity; FCS, functional connectivity strength; ReHo, regional homogeneity

pathophysiological changes and that (b) a reproducible functional signature of AD would be present across different scanner sites and detectable at the individual patient level. To assess the first hypothesis, we performed correlation analyses between altered functional measures and the Mini-Mental State Examination (MMSE) score and amyloid β (Aβ) burden. To assess the second hypothesis, we applied machine learning methods to conduct prediction tasks of individual diagnostic status and clinical score with leave-one-site-out cross-validation. Furthermore, we employed an independent dataset collected from the Alzheimer's Disease Neuroimaging Initiative (ADNI) to further validate the robustness of the main results of the present study.

2 | MATERIALS AND METHODS

2.1 | Participants, data and measurements

2.1.1 | Participants

The rs-fMRI data used in this study are described in detail elsewhere as part of a study investigating altered spontaneous activity in AD (Li et al., 2019; Zhao et al., 2020). Therefore, this section provides only a brief overview of the rs-fMRI acquisition, preprocessing and quality control, with further details in the supplemental material.

MRI was acquired in 688 individuals, including healthy comparison individuals (215) and individuals with MCI (221) and AD (252). Each individual was scanned with one of six different MRI scanners (Li et al., 2019). Demographic and clinical information stratified according to MRI site is shown in Table S2.

2.1.2 | Image acquisition and preprocessing

The MRI acquisition protocol is described in the supplementary material (Tables S3 and S4). Briefly, the resting-state fMRI scans were preprocessed using the Brainnetome Toolkit (http://brant.brainnetome.org) (Xu, Liu, Zhan, Ren, & Jiang, 2018), which included the following steps: (1) slice timing correction; (2) realignment to the first volume; (3) spatial normalization to Montreal Neurological Institute (MNI) space at 2 mm × 2 mm × 2 mm; (4) regression of nuisance signals, including linear trends, six motion parameters and their first-order differences, and signals representing white matter and cerebrospinal fluid; (5) temporal bandpass filtering (0.01–0.08 Hz) to reduce high-frequency noise. Subsequently, any voxel where the mean absolute deviation in the fMRI signal was less than 0.05 and any area that did not have fMRI signal recorded from one or more participants was excluded (Liu et al., 2014, 2016; Zhan et al., 2016).

The cortex and subcortex were parcellated based on the Brainnetome Atlas (Fan et al., 2016). The above preprocessing steps resulted in a set of 263 regional areas of the Brainnetome Atlas, which were used in all further analyses. The 263 regions comprising the parcellation atlas based on the overlapping regions of all the individuals are listed in the supplementary material (Table S7). We derived a regional fMRI signal for each region

by averaging the fMRI signal across all voxels included in the region. This process was repeated for all individuals and regions.

Additionally, the florbetapir (F18-AV-45) PET scans of 625 subjects (291 patients with AD and a well-matched [age and gender] group of 334 healthy comparison individuals) were collected from ADNI for subsequent correlation analysis. The downloaded F18-AV-45 PET images were already preprocessed, including computation of Standardized Uptake Value Ratio (SUVR) and smoothing. A detailed description of PET protocols and acquisition procedures can be found at (http://adni.loni.usc.edu/methods/pet-analysis-method/pet-analysis/). The PET images were rigidly co-registered to the corresponding T1 images and then nonlinearly co-registered to the standard MNI space at 2 mm × 2 mm × 2 mm by SPM12 (Statistical Parametric Mapping) software.

2.1.3 | Measure of functional brain activity and connectivity

In the present study, we used four measures of functional brain activity and connectivity derived from each individual's rs-fMRI data: amplitude of local brain activity (AM) (Liu et al., 2014), regional homogeneity (ReHo) (Zang, Jiang, Lu, He, & Tian, 2004), functional connectivity strength (FCS) (Sepulcre et al., 2010; Xia, et al., 2019) and whole-brain connectivity (Liu et al., 2014). Specifically, AM measures the magnitude of endogenous BOLD oscillations, quantified as the mean absolute value of the deviation of the BOLD fMRI signal from the mean value over the whole time series at a given voxel (Liu et al., 2014). ReHo measures the similarity or synchronization between the time series of a given voxel and its nearest neighbors (Zang et al., 2004), which is defined as the Kendall's coefficient of concordance of the time series of a given voxel and the time series of its K nearest neighbors. In this study, we used K = 27. FCS measures the total strength of functional coordination between a given voxel and all other voxels, that is, the sum of the strengths of functional connectivity beyond the threshold between a given voxel and all other voxels. In this study, connectivity strength was measured using Pearson's correlation coefficient, and the connectivity threshold was set to 0.2 (Sepulcre et al., 2010). Detailed definitions of these measures can be found in Table S8. Maps of AM, ReHo and FCS were estimated for each voxel and standardized within each subject to generate z-score maps, which could be appropriately averaged and compared across participants. We also computed functional connectivity between all pairs of regions, yielding a connectivity matrix for each individual. Regional estimates were calculated for each subject by averaging the z-scores of the voxels in each of the 263 brain regions.

2.2 | Group-level statistical analysis for identifying functional brain alterations in AD

2.2.1 | Meta-analysis across different sites

The null hypothesis of equality in AM, ReHo and FCS between the AD and healthy comparison groups was tested independently for each acquisition site. This hypothesis was also independently assessed using two sample two-sided t tests for the $(263 \times 262)/2$ = 34,453 unique functional connections. Age and gender were controlled using linear regression. In this way, functional connectivity and each of the three measures of activity (AM, ReHo, FCS) were associated with a p value for each of the acquisition sites and each brain region (or pair of brain regions in the case of functional connectivity). As suggested in previous studies, the Liptak-Stouffer z-score method was used to combine p values across the six sites, which has optimal power for combining probabilities in meta-analyses (Li et al., 2017; Xia, et al., 2019; Zaykin, 2011; Zhang et al., 2016; Zhao et al., 2020). Specifically, for each measure of brain activity (AM, ReHo and FCS) and connectivity, the p values for each dataset were transformed into z-scores using the inverse standard normal distribution. In particular, $z_i = \varphi^{-1}(1 - P_i/2)$, where φ is the standard normal cumulative distribution function. The combined z-score was then computed using the Liptak-Stouffer formula:

$$z = \frac{\sum_{i=1}^{k} w_i z_i}{\sqrt{\sum_{i=1}^{k} w_i{}^2}}$$

where w_i is the square root of the sample size of dataset i and k is the number of datasets (here, k = 6). Under the null hypothesis, the z-scores follow the standard normal distribution. Therefore, by converting the z-scores to p values, we identified significant regions (AM, ReHo and FCS) as well as significant connections that differed between the AD and healthy comparison groups. The Bonferroni correction was used to correct for multiple comparisons across the set of all 263 regions (p < .05, N = 263 for AM, ReHo and FCS) and the set of 34,453 functional connections) (Li et al., 2017; Zhang et al., 2016). In addition, we also performed a meta-analysis between MCI and healthy individuals, and between AD and MCI for each of the four measures.

2.2.2 | Post hoc clustering and correlation analysis

To extend the above analyses and provide further insight into the network abnormality of AD from the perspective of network circuits and hubs, we performed a spectral clustering analysis of functional connectivity (Figure 1). The similarity matrix was obtained from the Pearson's correlation coefficient of each pair of altered connections that were identified through the above meta-analysis in AD patients. The similarity represented the degree of covariation across the AD individuals between each pair of functional connections that were found to show a significant between-group difference (Skatun et al., 2017). This measure of covariance quantifies whether functional connectivity strength remains consistent across individuals and does not require connectivity to decrease or increase consistently (Skatun et al., 2017). Hence, this measure is more appropriate to detect network circuits and alleviate potential errors caused by individual differences.

To determine whether the above meta-analyses identified altered functional measures that associated with cognitive impairment in the AD and MCI individuals (here with the MCI subjects were included to test whether a disease severity association exists), we performed Pearson's correlation analysis between each of four measures (AM, ReHo, FCS and functional connectivity) and the severity of cognitive impairment as measured by MMSE scores of AD/MCI ($p < .05$, false discovery rate [FDR] corrected). Note that the correlation analysis between four measures and the MMSE were performed only on regions or functional connections with significant group differences between AD and NC (healthy individuals). The effects of age, gender and scanner site were controlled. Additionally, we performed Pearson correlation analysis between the mean functional connectivity strength of each cluster and the MMSE scores of AD/MCI ($p < .05$, Bonferroni correction for cluster numbers).

To determine whether the extent of AD-related abnormalities in functional activity associates with the extent of Aβ burden, we performed correlation analysis between case–control differences in each of four functional measures (AM, ReHo FCS and functional connectivity) as quantified by the z-statistics of the above meta-analyses and case–control differences of Aβ burden (z-score) as quantified by statistics of two-sample two-sided t test ($p < .05$, Bonferroni correction for four measures) with age, gender, gray matter volume controlled. Regional levels of Aβ burden were determined using florbetapir (F18-AV-45) PET scans collected from ADNI (detailed in Table S5). A t statistic quantifying the Aβ burden for each of 263 regions was determined using two sample two-sided t test between 291 patients with AD and a well-matched (age and gender) group of 334 healthy comparison individuals. Note that increased amyloid pathology corresponded to a positive t statistic value.

2.3 | Multivariate classification and prediction based on functional activity and connectivity

To assess the predictive utility of the fMRI measures considered in this study, we performed classification analysis and regression analysis using leave-one-site-out cross-validation (Abraham et al., 2017; Nunes et al., 2018; Rozycki et al., 2018). To evaluate the generalizability of the classifier across sites, we trained a linear support vector machine (SVM) classifier to predict individual diagnostic status (AD vs. healthy comparison individual); to investigate the generalization of the regression models, an ElasticNet regression model was introduced to predict individual clinical MMSE scores (https://scikitlearn.org/stable/modules/linear_model.html#elastic-net) (Friedman, Hastie, & Tibshirani, 2010; Schouten et al., 2016; Zou & Hastie, 2005). The input features for the classification and regression models were selected based on repeating the meta-analyses described above on the five excluded training sites. For each iteration of the cross-validation, this yielded a feature space that comprised AM, ReHo, FCS and functional connectivity measures. The accuracy of the classifier was then evaluated on the individuals comprising the remaining site that was not used during the feature selection process, giving rise to a sixfold cross-validation process in which one site served as the testing set for each fold (Figure S1). Briefly, as Figure S1 shows, for each validation fold, we firstly selected one site as the testing set and other five sites as the training set. Second, we achieved four functional measures of subjects on training set and conducted meta-analysis of each of the four measures. Third, we selected the features with significant group differences between AD and NC surviving the FDR correction ($p < .05$) to train a classification model and a regression model. The SVM and ElasticNet hyperparameters of models are optimized by inner fivefold cross-validation on the training set (parameter candidates are listed in the Tables S11 and S12). Finally, we computed the corresponding functional measures on testing set to predict the diagnosis state and MMSE score of subject by the trained models. Classification performance was evaluated using accuracy (ACC), sensitivity (SEN), specificity (SPE) and area under the receiver operating characteristic curve (AUC) (Feng et al., 2018; Lian, Liu, Zhang, & Shen, 2020; Liu, Zhang, Adeli, & Shen, 2018; Rozycki et al., 2018). Prediction performance was evaluated using the Pearson correlation coefficient and mean absolute error (MAE) between the actual and the predicted MMSE (Stonnington et al., 2010).

2.4 | Replication of main results on the ADNI database

To further validate the robustness of the main results of the present study, an independent dataset with 39 patients with AD and a well-matched (age and gender) group of 45 healthy individuals was included for replication analysis from the ADNI (www.loni.ucla.edu/ADNI). Of the 39 patients with AD, 23 subjects had at least three longitudinal scans (Table S6). The same quality control criteria and preprocessing pipeline described above were applied to the ADNI database. After that, we performed a two-sample two-sided t test analysis on each measure (AM, ReHo, FCS and whole-brain connectivity) between the AD and healthy comparison groups with age and gender controlled. Then, correlation analyses between the primary database and the ADNI database were performed for each measure to investigate whether the pattern of between-group differences were regionally consistent between the two datasets. Additionally, to test whether the functional connectivity strength changes significantly with the course of disease, we performed one-way repeated-measures analysis of variance (ANOVA) for each of the identified clusters from the ADNI database on the longitudinal data (23 AD patients with three scans).

Additionally, we trained an SVM classification model for AD diagnosis on the primary database and tested it on the ADNI database. The features were selected with significant group differences between AD and NC above meta-analysis of the primary database.

2.5 | Features and code sharing

The open Brainnetome fMRI toolkit (Xu et al., 2018) is available online at https://github.com/yongliulab. The SVM and regression analysis code used

in this study can be obtained at https://scikit-learn.org/. The data used are available from the author (Y.L.) upon reasonable request.

3 | RESULTS

3.1 | Regional and connectivity analyses reveal replicated brain abnormalities in AD

3.1.1 | Altered functional activity in AD

Meta-analyses were performed to test for differences in measures of functional activity between six cohorts of individuals with AD and corresponding healthy comparison individuals. The quantitative comparison results of group difference between AD patients and corresponding healthy comparison individuals for each of the six centers using *t* test are shown in Figure S2. Figure 2a shows cortical maps that indicate regions associated with significant differences in AM, ReHo and/or FCS between the AD and healthy comparison groups ($p < .05$, Bonferroni corrected for $N = 263$ regional comparisons). Whereas some regions were found to show significant increases in these three measures of functional activity, other regions were associated with significant decreases in the AD group compared to the healthy comparison group. Importantly, a consistent regional pattern of significant AD-related alterations in functional activity was evident across the three measures, principally circumscribed to the default-mode network (DMN), including the posterior cingulate cortex, precuneus, inferior parietal lobule, hippocampus, thalamus, and fusiform gyrus (Figure 2a and Table S9). Specifically, the AD group was associated with significantly reduced functional activity in the precuneus, inferior parietal lobule (AM, ReHo, FCS), posterior cingulate cortex and middle frontal gyrus (AM, ReHo), superior frontal gyrus (ReHo) and anterior superior temporal sulcus (FCS). In addition, the AD group showed significantly higher functional activity in the fusiform gyrus, hippocampus, parahippocampal gyrus and superior temporal gyrus (AM, ReHo), the thalamus and cerebellum (ReHo, FCS), the amygdala (AM), the basal ganglia (ReHo) and middle frontal gyrus (FCS).

3.1.2 | Altered whole-brain functional connectivity in AD

Meta-analyses were performed to test for differences in functional connectivity strength associated with AD across all pairs of regions comprising the Brainnetome Atlas. We found 178 functional connections with reduced connectivity strength in the AD group and 38 connections with increased strength relative to the healthy comparison group ($p < .05$, Bonferroni corrected, $N = 34{,}453$ connection comparisons) (Figure 3, Table S10, Figure S3). To identify the key regions impacted by these functional connectivity alterations, we used spectral clustering to group the altered connections into putative clusters based on covariance across the group of AD individuals. The connections that showed significant reductions in functional connectivity in the AD group were divided into four clusters according to the silhouette coefficient (https://scikit-learn.org/stable/modules/clustering.html#clustering) (cluster 1–4, Figure 3b, Figure S4). Fewer connections were associated with significant increases in functional connectivity in the AD group, and all of these connections were assigned to a single cluster (cluster 5). The cluster analysis indicated that reductions in connectivity strength primarily involved the DMN, cingulate gyrus, basal ganglia and lateral occipital cortex, whereas increased connectivity was limited to the prefrontal lobe (Figure 3). As shown in Figure 3b, cluster 1 contained connections that belong to the DMN, especially connections between the frontal lobe and temporal lobe, and connections between the temporal lobe and precuneus. Cluster 2 comprised connections between the anterior cingulate cortex and other regions, especially the parietal lobe. Cluster 3 contained some connections between the occipital lobe and temporal lobe and connections between the occipital lobe and cingulate gyrus. Cluster 4 comprised connections between the basal ganglia, association cortex and subcortical structures.

In addition, the results of regions with significant group differences between MCI and NC, and between AD and MCI with Bonferroni correction ($p < .05$) are shown in Figure S5. After that, we performed correlation analysis between the *z* scores of differences between AD and NC and the *z* scores of differences between MCI and NC, between the *z* scores of differences between AD and NC and the *z* scores of differences between AD and MCI for four measures. The results showed that the changes in difference of three groups are consistent (all $p < 10E\text{-}30$) (Figure S5).

3.1.3 | Associations between functional activity/connectivity and clinical scores in AD and MCI

Correlation analyses were undertaken to determine whether inter individual variation in symptom severity associated with fMRI measures in regions with significant changes in each measure ($N = 44$ for AM, $N = 79$ for ReHo, $N = 19$ for FCS) and functional connections showing between-group differences ($N = 226$) ($p < .05$, FDR corrected for N comparisons). The correlation analysis was performed in the combined AD and MCI groups and each of two groups after controlling for the effects of age, gender and center, also the MCI and AD group respectively (Tables S9 and S10). Functional measures in the inferior parietal lobule (AM, ReHo, FCS), precuneus and cingulate gyrus (AM, ReHo), and middle frontal gyrus (ReHo) showed significant positive correlations with the MMSE scores in the combined AD and MCI groups (Table S9). Functional measures in the fusiform gyrus and hippocampus (AM, ReHo), thalamus and cerebellum (ReHo, FCS), superior temporal gyrus and basal ganglia (ReHo) showed significant negative correlations with MMSE scores in the combined AD and MCI groups (Figure 2d–f). Importantly, 162 functional connections (71.7%) were significantly correlated with MMSE scores in the combined AD and MCI groups ($p < .05$, FDR corrected, Table S10). In addition, we also performed correlation analysis between the mean functional connectivity strength of each of the five identified clusters and MMSE scores in AD and MCI ($p < .05$, FDR corrected). As shown in Figure 3b, there were significant positive correlations between

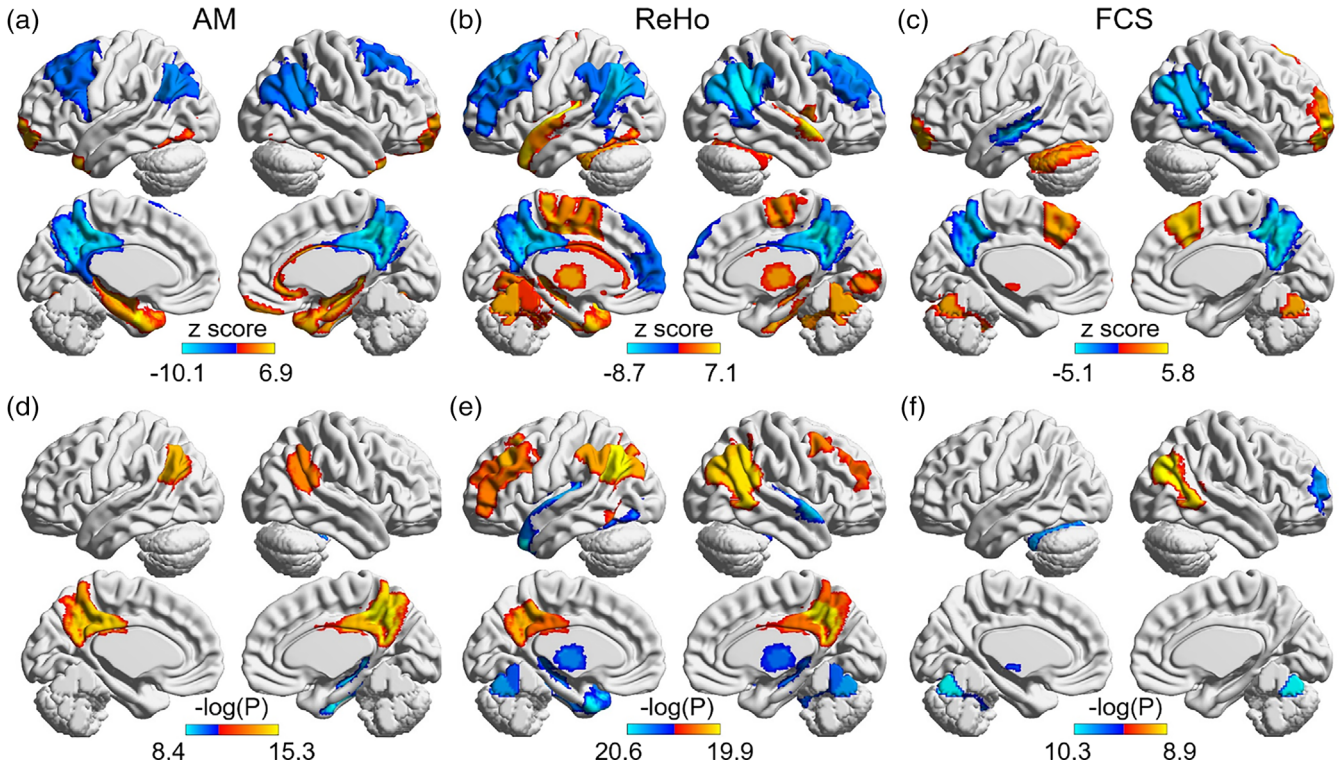

FIGURE 2 (a–c) Differences in functional measures (AM, ReHo and FCS) between patients with AD and healthy controls. The warmer and colder colors indicate higher and lower functional measures in patients with AD than in the healthy controls, respectively. (d–f) The correlation map between altered functional measures (AM, ReHo, FCS) and MMSE scores in the AD and MCI patients with FDR correction ($p < .05$). AD, Alzheimer's disease; AM, the amplitude of local brain activity; FCS, functional connectivity strength; MCI, mild cognitive impairment; MMSE, Mini-Mental State Examination; ReHo, regional homogeneity

mean functional connectivity strength and the MMSE scores for clusters 1–4 ($p < .001$). In contrast, the mean functional connectivity strength of cluster 5, which contained significantly increased connectivity in AD compared to the healthy comparison group, was negatively correlated with MMSE scores ($p < .001$). The case–control differences in ReHo and FCS (AM has no significant result $p = .88$) were significantly associated with another independent case–control difference in Aβ burden, which shows that the abnormalities in functional activity are associated with pathological changes related to AD.

3.2 | Multivariate classification and prediction based on functional activity and connectivity

Using a cross-validation process, we trained machine learning classifiers to predict diagnostic status and clinical MMSE score based on an individual's AM, ReHo, FCS and functional connectivity (details of parameter candidates are listed in the supplemental material). For each iteration of cross-validation, the site chosen to test the performance of the trained classifier was never used as part of the feature selection process and classifier training. Diagnostic status could be predicted with a relatively high AUC of 0.95 (ACC = 0.89, SEN = 0.86, SPE = 0.95) (Figure 4a; the classification results of each test dataset were summarized in Table S11). More significantly, we found significant negative correlations ($r = -.32$, $p < .001$ for AD, $r = -.29$, $p < .001$ for MCI, and $r = -.43$, $p < .001$ for AD and MCI) between the individual pseudoprobabilities of AD and MCI subjects and cognitive ability (Figure 4b). For disease progression, the mean correlation coefficient and MAE between the predicted and actual MMSE scores of the six test sets were 0.56 ($p < .001$) and 4.37, respectively (Figure 4c). The prediction results of each test set were summarized in Table S12. Furthermore, the classification accuracy of the model trained on the primary database and tested on the ADNI database is 0.70 (AUC = 0.73, SEN = 0.82, SPE = 0.60). Taken together, these results emphasized the potential for brain activity and connectivity to provide a robust and reproducible imaging signature of AD.

3.3 | Generalization of the altered activity in AD

3.3.1 | Replication of main results using the ADNI database

We performed a two-sample two-sided t test between the AD and healthy comparison groups in the ADNI database after controlling for the effects of age and gender with AM, ReHo and FCS. To investigate whether there is a similar pattern of case–control difference across the two databases, we performed a correlation analysis between the z statistic of the meta-analysis of the primary database and the

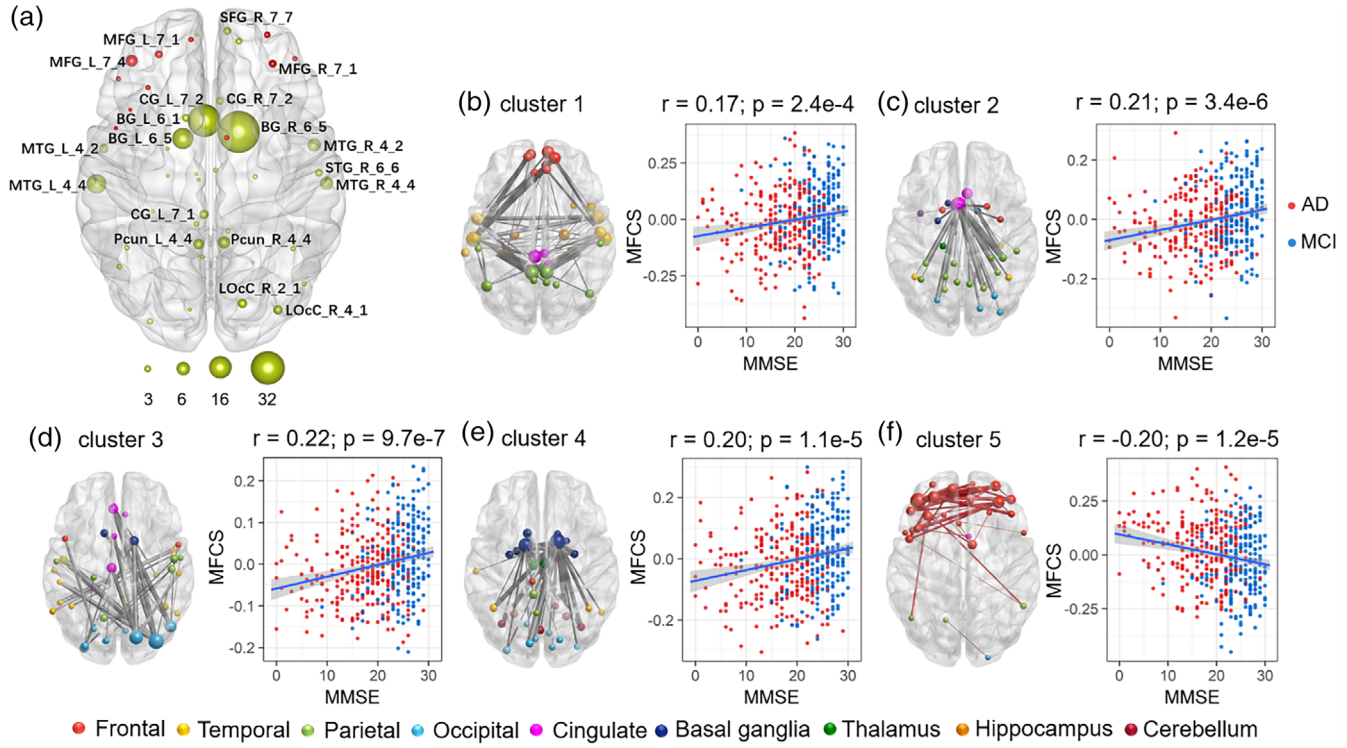

FIGURE 3 (a) The main affected regions with more than two altered connections are shown in the left upper. The size of the node represents the number of altered connections in the brain region. Nodes in red color and yellow color indicate the region involved in enhanced and attenuated connectivity, respectively; (b–f) the spectral clustering results of altered functional connections and the scatter plot of significant association between mean functional connectivity strength and the MMSE scores in the AD and MCI patients for five clusters ($p < .001$). AD, Alzheimer's disease; MCI, mild cognitive impairment; MMSE, Mini-Mental State Examination

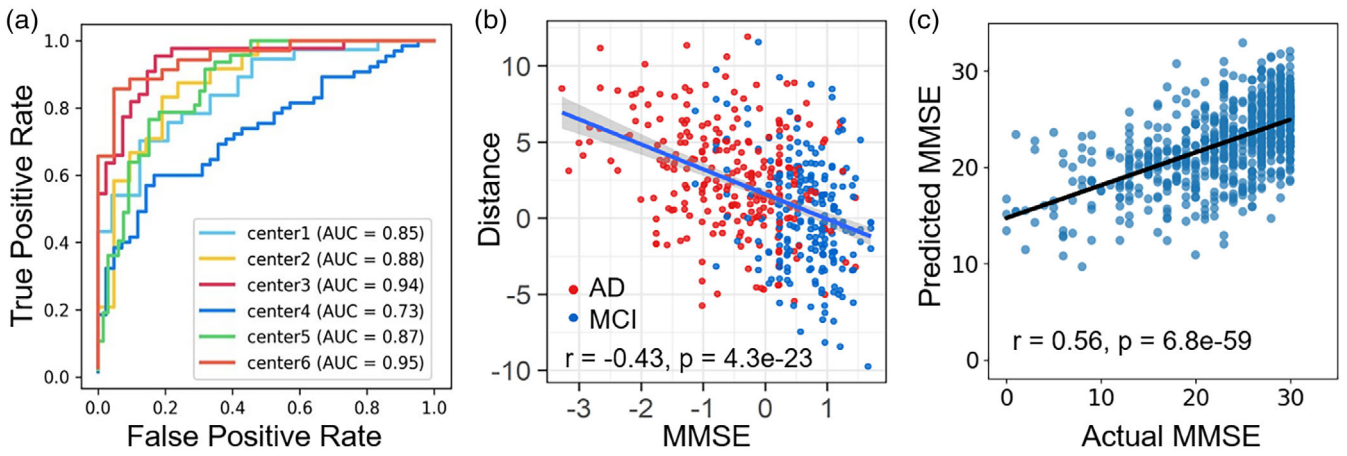

FIGURE 4 (a) The receiver operating characteristic curves (ROC) and area under ROCs (AUC) of intersite cross-validations. (b) Correlation between the distances of the test samples from the discrimination hyperplane and MMSE scores. MMSE scores were *z*-scored within each dataset and then pooled together. The results showed significant negative correlations ($r = -.32$, $p = 1.4e^{-7}$ for AD, $r = -.29$, $p = 9.0e^{-6}$ for MCI, $r = -.43$, $p = 4.3e^{-23}$ for AD plus MCI) between the individual pseudoprobabilities of AD and MCI subjects and the cognitive ability. (c) The correlation between predicted and actual MMSE scores of six sites using leave-one-site-out cross-validation. AD, Alzheimer's disease; MCI, mild cognitive impairment; MMSE, Mini-Mental State Examination

t statistic of the *t* test of the ADNI database with AM, ReHo, FCS and functional connectivity after controlling for the effects of age and gender (Tables S6 and S13). Patterns of abnormalities were spatially consistent between the two databases (whole-brain functional connectivity: $r = .20$, $p < .001$; AM: $r = .35$, $p < .001$; ReHo: $r = .63$, $p < .001$; FCS: $r = .16$, $p = .008$; Figure 5). Specifically, the AD group

had significantly higher functional activities in the fusiform gyrus and superior temporal gyrus (AM, ReHo, FCS) ($p < .05$, Bonferroni correction). In addition, the AD group exhibited significantly lower FCS in the insular. The identified regions of the fusiform gyrus and superior temporal gyrus were consistent with our main results.

To test whether the functional connectivity strength changes significantly with the course of disease, we performed one-way repeated measures ANOVA for each of five identified clusters in AD patients. Strikingly, the connectivity strength of cluster 2 (e.g., the anterior cingulate, $F = 4.42$, $p = .018$ uncorrected) and cluster 4 (e.g., basal ganglia, $F = 3.46$, $p = .04$ uncorrected) changed significantly with time in the longitude AD subjects (Table S14). These additional findings provided further evidence for the robustness and reproducibility of the present findings.

3.3.2 | Control analyses

First, we tested the robustness of our main findings to alternative parcellation atlases. As a control analysis for the choice of brain parcellation, at a regional scale, we repeated the analysis to identify comparable differences between the AD and healthy comparison groups using the Stanford Atlas (http://findlab.stanford.edu/functional_ROIs.html) (Richiardi et al., 2015) (Further details are provided in Figure S6).

Second, to investigate the potential confound of different acquisition lengths across the six sites, we temporally truncated the fMRI data for all individuals across all six sites to the shortest acquisition (170 time points). The results showed that the temporal truncation step (keeping the first 170 time points for each subject) did not alter the patterns of impaired functional activity and connectivity in the AD group (Figures S7 and S8).

4 | DISCUSSION

To the best of our knowledge, this is the first data-driven meta-analysis study to directly investigate aberrant brain activity and dysfunction of whole-brain networks in AD with a large database pooled across six sites. Our study provided a comprehensive picture and strong evidence for a pattern of widespread functional

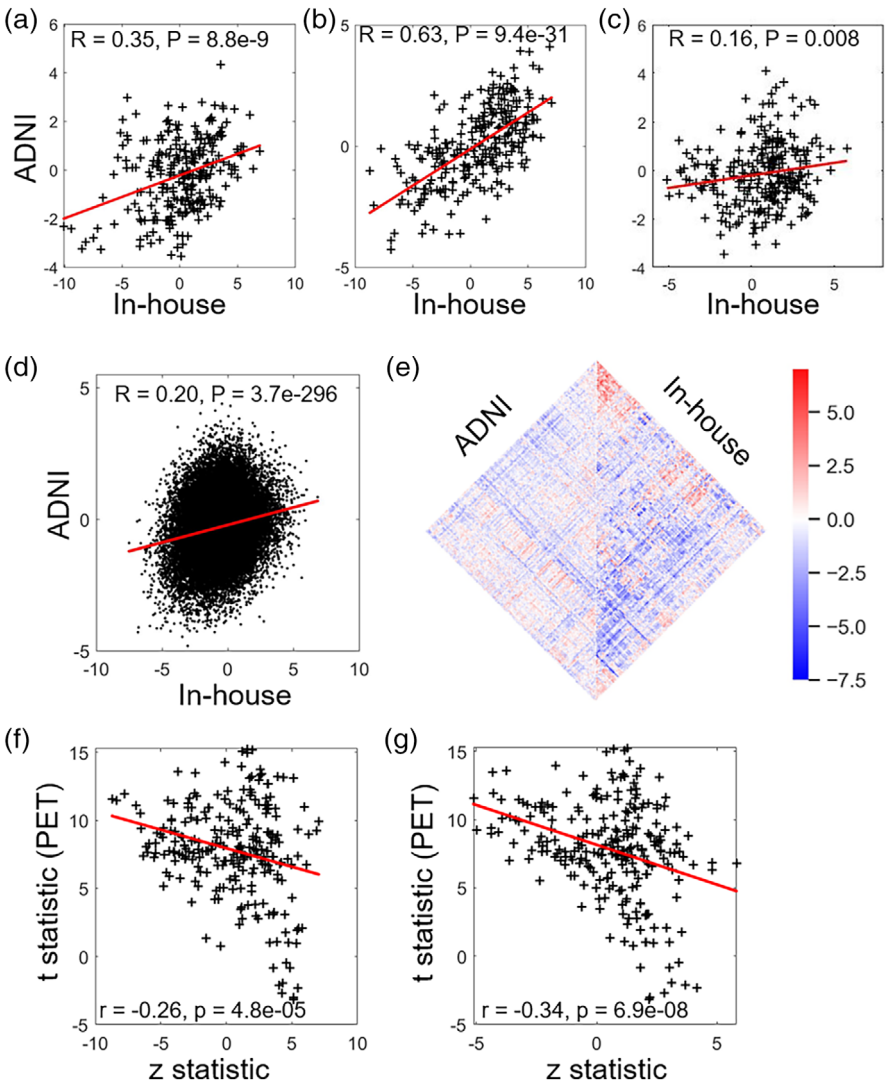

FIGURE 5 Correlation analysis of the case–control difference between the primary database and the ADNI database. The correlation analysis between z statistic of functional measures (AM (a), ReHo (b), FCS (c), functional connectivity (d)) by meta-analyses on the primary database and *t* statistic of functional measures by two-sample *t* test on the ADNI database after controlling for the effects of age and gender. (e) The heatmap of the case–control difference of functional connectivity of the ADNI database and primary database. The correlation analysis between the z statistic of ReHo (f) and FCS (g) measures on the primary database and the *t* statistic of the Aβ burden on the ADNI database. AM, the amplitude of local brain activity; ReHo, regional homogeneity; FCS, functional connectivity strength; Aβ, amyloid β

dysconnectivity in AD, enabling accurate individual prediction of diagnostic status and clinical score. More specifically, patients with AD consistently displayed reduced brain activity within the DMN and increased activity located in subcortical nuclei, particularly the hippocampus, parahippocampus, amygdala and thalamus. For whole-brain network dysconnectivity, patients with AD consistently displayed reduced connectivity or activity involving the DMN, basal ganglia, and cingulate gyrus. In contrast, the prefrontal lobe displayed hyperconnectivity in AD. Interindividual variation in the severity of these abnormalities was significantly correlated with the severity of cognitive impairment and Aβ burden determined from an independent group of individuals. Taken together, these findings deepened our understanding of brain dysfunction in AD.

We confirmed that AD is associated with hypoconnectivity and aberrant brain activity in the DMN, a network playing a pivotal role in various cognitive functions, emotional processing and retrieval of episodic memory. The DMN is also involved in the integration and communication of information from other brain regions (Seguin, Razi, & Zalesky, 2019), which were primarily impaired for AD (Eyler et al., 2019; Raichle et al., 2001). The present findings suggest that the regional distribution of AD deficits is circumscribed to well-defined canonical networks. In particular, Aβ deposition, hypometabolism, and gray matter atrophy have all been found to be regionally circumscribed to core regions of the DMN (Dickerson et al., 2009; Grothe, Teipel, & Alzheimer's Disease Neuroimaging, 2016). The significant spatial association between Aβ deposition and dysfunction inferred from rs-fMRI suggests that these functional deficits have an underlying neurobiological basis. We also found that AD exhibited hypoconnectivity among the anterior cingulate cortex and basal ganglia. The basal ganglia, cerebellum and cerebral cortex form an integrated network that is involved in motor, cognition and emotion and provides an important component of the substrate for multiple intrinsic resting-state networks (Alexander, DeLong, & Strick, 1986; Bostan & Strick, 2018; Habas et al., 2009; Postuma & Dagher, 2006). Residing at the junction of a wide cortico-subcortical network, the anterior cingulate cortex is associated with complex functions that are known to be abnormal in AD, such as emotions, motor control and cognition (Apps, Rushworth, & Chang, 2016; MacDonald 3rd, Cohen, Stenger, & Carter, 2000; Mega & Cummings, 1997; Paus, 2001). Additionally, anterior cingulate cortex hypofunction is closely associated with apathy and unawareness of deficits, which are common neuropsychiatric symptoms in patients with AD (Amanzio et al., 2011; Marshall et al., 2007).

Notably, we found evidence suggesting that AD is associated with short-distance hyperconnectivity within the prefrontal cortex. This may point to a compensatory mechanism to offset functional impairments due to disconnection between multiple other regions (Bai et al., 2009; Becker et al., 1996; Gould et al., 2006; Grady et al., 2003; Qi et al., 2010). Interestingly, we also observed that the hippocampus, parahippocampus and thalamus showed increased local activity strength when combined with decreased functional connectivity with other brain regions (Figures 2 and 3). These local increases may lead to functional decoupling with distant regions.

The development of valid biomarkers is crucial for optimizing individualized care in AD. Thus, identifying reproducible and generalizable markers is essential for the AD research community. It should be noted that there is a lack of the verification of reproducibility and the evaluation of functional imaging characteristics as diagnostic biomarkers due to small sample sizes in most of the previous studies. We employed a large fMRI biobank and applied the same analysis pipeline to investigate AD-relevant functional alterations, which successfully reduce the methodological variability, biased sampling and further improve statistical power. To our knowledge, this study included the largest rs-fMRI AD biobank collected in China. The large sample size ensures that the present findings are reproducible (Varoquaux, 2018). The additional control analyses (different parcellation methods, different time series lengths and an independent ADNI database) highlighted the reproducibility of the imaging signatures identified in this study and provide further support for the robustness of the present results. Additionally, significant associations between functional measures and clinical scores and amyloid-β burden in an independent database deepen our understanding of the neuropathology of AD. The multivariate analysis with cross-validation further supported the clinical benefits of functional measures, which is valuable for clinical decision-making and therapeutic development. These findings demonstrated that the spontaneous activity pattern can provide robust and generalized imaging biomarkers across sites (Abraham et al., 2017; Rozycki et al., 2018; Teipel et al., 2017), and this kind of generalizability is particularly important for translational medicine (Davatzikos, 2019).

This study has several limitations that should be considered. First, it should be noted that the image acquisition scanning protocols differed across the studied sites. Instead of directly pooling data from multiple sites, we performed statistical comparisons for each site and combined the results though meta-analysis to attenuate the effects of these confounds. The variations in scanning parameters (such as, field of view, echo time, slice numbers) have an unknown effect on present results to some degree, this might explain the relatively modest accuracy when using ADNI as the validation dataset. It would be better to minimize the inconsistencies in the image parameters for group analyses in future multisite studies by leveraging harmonization techniques (Yu et al., 2018; Zhou, et al., 2018). Second, longitudinal datasets or associations with Aβ burden directly were not available in this study. Future studies are also needed to include longitudinal neuroimaging and neurobiological data to further verify the reproducibility of AD-relevant functional alterations and develop reliable biomarkers for the progression of AD. Third, in this study, we only focus on the robustness of aberrant patterns of brain activity and the diagnostic utility of fMRI measures in AD. Neuroimaging-based classification of AD with other modalities, such as structural MRI and PET, achieved promising classification performance (Rathore, Habes, Iftikhar, Shacklett, & Davatzikos, 2017). One single neuroimaging modality cannot be sufficient to completely characterize alterations in the brains of AD. For better quantitative diagnosis, multimodal techniques and new machine learning protocols that elucidate distinctive imaging signatures are needed for early diagnosis and prediction.

Lastly, we need to develop suitable machine learning method for early detection and progress detection of the MCI subjects.

5 | CONCLUSION

To the best of our knowledge, this is the first mega-analysis study to comprehensively examine functional alterations in individuals with AD using a large multicenter rs-fMRI database (N = 688). More specifically, aberrant connectivity and local activity in the DMN, cingulate gyrus, basal ganglia, and hippocampus may underlie AD biases toward cognition and communication of information. The control analysis further supported the reproducibility of our findings. Inter individual variation in the severity of these functional abnormalities was significantly correlated with the degree of cognitive impairment and Aβ burden, which deepened our understanding of the association between neuropathology and activity dysfunction of AD. Predictions of an individual's diagnostic status and clinical score indicated the potential of functional signatures as biomarkers or predictors of disease progression in AD. Collectively, these reproducible and generalizable findings highlighted the potential for functional brain imaging biomarkers in the early diagnosis of AD.

ACKNOWLEDGMENTS

This work was partially supported by the National Key Research and Development Program of China (grant nos. 2016YFC1305904, 2018YFC2001700), the National Natural Science Foundation of China (grant nos. 81871438, 81901101, 61633018, 81571062, 81701781), the Strategic Priority Research Program (B) of the Chinese Academy of Sciences (grant no. XDB32020200) and the Beijing Municipal Sciences & Technology Commission (grant nos. Z171100000117001). Replicated ADNI data collection and sharing were funded by the ADNI (National Institutes of Health Grant U01 AG024904) and DOD ADNI (Department of Defense award number W81XWH-12-2-0012). ADNI is funded by the National Institute on Aging, the National Institute of Biomedical Imaging and Bioengineering, and through generous contributions from the following: AbbVie, Alzheimer's Association; Alzheimer's Drug Discovery Foundation; Araclon Biotech; BioClinica, Inc.; Biogen; Bristol-Myers Squibb Company; CereSpir, Inc.; Cogstate; Eisai Inc.; Elan Pharmaceuticals, Inc.; Eli Lilly and Company; EuroImmun; F. Hoffmann-La Roche Ltd. and its affiliated company Genentech, Inc.; Fujirebio; GE Healthcare; IXICO Ltd.; Janssen Alzheimer Immunotherapy Research & Development, LLC.; Johnson & Johnson Pharmaceutical Research & Development LLC.; Lumosity; Lundbeck; Merck & Co., Inc.; Meso Scale Diagnostics, LLC.; NeuroRx Research; Neurotrack Technologies; Novartis Pharmaceuticals Corporation; Pfizer Inc.; Piramal Imaging; Servier; Takeda Pharmaceutical Company; and Transition Therapeutics. The Canadian Institutes of Health Research is providing funds to support ADNI clinical sites in Canada. Private sector contributions are facilitated by the Foundation for the National Institutes of Health (www.fnih.org). The grantee organization is the Northern California Institute for Research and Education, and the study is coordinated by the Alzheimer's Therapeutic Research Institute at the University of Southern California. ADNI data are disseminated by the Laboratory for Neuro Imaging at the University of Southern California. The funder of the study had no role in study design, data collection, data analysis, data interpretation, or writing of the report. The authors report no biomedical financial interests or potential conflicts of interest. The corresponding author had full access to all the data in the study and had final responsibility for the decision to submit for publication. We thank Dr. Han Zhang for his critical discussions and comments.

DATA AVAILABILITY STATEMENT

All computer code used to identify our biomarker and the preprocessed fMRI results will be made freely available https://github.com/YongLiuLab

ORCID

Nianming Zuo https://orcid.org/0000-0002-6726-4575
Jie Lu https://orcid.org/0000-0003-0425-3921
Tianzi Jiang https://orcid.org/0000-0001-9531-291X
Yong Liu https://orcid.org/0000-0002-1862-3121

REFERENCES

Abraham, A., Milham, M. P., Di Martino, A., Craddock, R. C., Samaras, D., Thirion, B., & Varoquaux, G. (2017). Deriving reproducible biomarkers from multi-site resting-state data: An autism-based example. *NeuroImage*, *147*, 736–745.

Academy of Cognitive Disorders of China, Han, Y., Jia, J., Li, X., Lv, Y., Sun, X., … Zhou, Y. (2020). Expert consensus on the care and Management of Patients with cognitive impairment in China. *Neuroscience Bulletin*, *36*, 307–320.

Alexander, G. E., DeLong, M. R., & Strick, P. L. (1986). Parallel organization of functionally segregated circuits linking basal ganglia and cortex. *Annual Review of Neuroscience*, *9*, 357–381.

Amanzio, M., Torta, D. M., Sacco, K., Cauda, F., D'Agata, F., Duca, S., … Geminiani, G. C. (2011). Unawareness of deficits in Alzheimer's disease: Role of the cingulate cortex. *Brain*, *134*, 1061–1076.

Apps, M. A., Rushworth, M. F., & Chang, S. W. (2016). The anterior cingulate gyrus and social cognition: Tracking the motivation of others. *Neuron*, *90*, 692–707.

Bai, F., Liao, W., Watson, D. R., Shi, Y., Wang, Y., Yue, C., … Zhang, Z. (2011). Abnormal whole-brain functional connection in amnestic mild cognitive impairment patients. *Behavioural Brain Research*, *216*, 666–672.

Bai, F., Watson, D. R., Yu, H., Shi, Y., Yuan, Y., & Zhang, Z. (2009). Abnormal resting-state functional connectivity of posterior cingulate cortex in amnestic type mild cognitive impairment. *Brain Research*, *1302*, 167–174.

Becker, J. T., Mintun, M. A., Aleva, K., Wiseman, M. B., Nichols, T., & DeKosky, S. T. (1996). Compensatory reallocation of brain resources supporting verbal episodic memory in Alzheimer's disease. *Neurology*, *46*, 692–700.

Bostan, A. C., & Strick, P. L. (2018). The basal ganglia and the cerebellum: Nodes in an integrated network. *Nature Reviews. Neuroscience*, *19*, 338–350.

Braak, H., & Braak, E. (1991). Neuropathological stageing of Alzheimer-related changes. *Acta Neuropathologica*, *82*, 239–259.

Bullmore, E., & Sporns, O. (2012). The economy of brain network organization. *Nature Reviews. Neuroscience*, *13*, 336–349.

Button, K. S., Ioannidis, J. P., Mokrysz, C., Nosek, B. A., Flint, J., Robinson, E. S., & Munafo, M. R. (2013). Power failure: Why small

sample size undermines the reliability of neuroscience. *Nature Reviews. Neuroscience*, *14*, 365–376.

Costafreda, S. G. (2009). Pooling FMRI data: Meta-analysis, mega-analysis and multi-center studies. *Frontiers in Neuroinformatics*, *3*, 33.

Davatzikos, C. (2019). Machine learning in neuroimaging: Progress and challenges. *NeuroImage*, *197*, 652–656.

Delbeuck, X., Collette, F., & Van der Linden, M. (2007). Is Alzheimer's disease a disconnection syndrome? Evidence from a crossmodal audio-visual illusory experiment. *Neuropsychologia*, *45*, 3315–3323.

Delbeuck, X., Van der Linden, M., & Collette, F. (2003). Alzheimer's disease as a disconnection syndrome? *Neuropsychology Review*, *13*, 79–92.

Dennis, E. L., & Thompson, P. M. (2014). Functional brain connectivity using fMRI in aging and Alzheimer's disease. *Neuropsychology Review*, *24*, 49–62.

Dickerson, B. C., Bakkour, A., Salat, D. H., Feczko, E., Pacheco, J., Greve, D. N., … Buckner, R. L. (2009). The cortical signature of Alzheimer's disease: Regionally specific cortical thinning relates to symptom severity in very mild to mild AD dementia and is detectable in asymptomatic amyloid-positive individuals. *Cerebral Cortex*, *19*, 497–510.

Eickhoff, S. B., Yeo, B. T. T., & Genon, S. (2018). Imaging-based parcellations of the human brain. *Nature Reviews. Neuroscience*, *19*, 672–686.

Eyler, L. T., Elman, J. A., Hatton, S. N., Gough, S., Mischel, A. K., Hagler, D. J., … Kremen, W. S. (2019). Resting state abnormalities of the default mode network in mild cognitive impairment: A systematic review and meta-analysis. *Journal of Alzheimer's Disease*, *70*, 107–120.

Fan, L., Li, H., Zhuo, J., Zhang, Y., Wang, J., Chen, L., … Jiang, T. (2016). The human Brainnetome atlas: A new brain atlas based on connectional architecture. *Cerebral Cortex*, *26*, 3508–3526.

Feng, F., Wang, P., Zhao, K., Zhou, B., Yao, H., Meng, Q., … Liu, Y. (2018). Radiomic features of hippocampal subregions in Alzheimer's Disease and amnestic mild cognitive impairment. *Frontiers in Aging Neuroscience*, *10*, 290.

Filippi, M., Basaia, S., Canu, E., Imperiale, F., Meani, A., Caso, F., … Agosta, F. (2017). Brain network connectivity differs in early-onset neurodegenerative dementia. *Neurology*, *89*, 1764–1772.

Fornito, A., & Bullmore, E. T. (2015). Connectomics: A new paradigm for understanding brain disease. *European Neuropsychopharmacology*, *25*, 733–748.

Friedman, J., Hastie, T., & Tibshirani, R. (2010). Regularization paths for generalized linear models via coordinate descent. *Journal of Statistical Software*, *33*, 1–22.

Gauthier, S., Reisberg, B., Zaudig, M., Petersen, R. C., Ritchie, K., Broich, K., … International Psychogeriatric Association Expert Conference on mild cognitive, i. (2006). Mild cognitive impairment. *Lancet*, *367*, 1262–1270.

Gould, R. L., Arroyo, B., Brown, R. G., Owen, A. M., Bullmore, E. T., & Howard, R. J. (2006). Brain mechanisms of successful compensation during learning in Alzheimer disease. *Neurology*, *67*, 1011–1017.

Grady, C. L., McIntosh, A. R., Beig, S., Keightley, M. L., Burian, H., & Black, S. E. (2003). Evidence from functional neuroimaging of a compensatory prefrontal network in Alzheimer's disease. *The Journal of Neuroscience*, *23*, 986–993.

Grothe, M. J., Teipel, S. J., & Alzheimers Disease Neuroimaging, I. (2016). Spatial patterns of atrophy, hypometabolism, and amyloid deposition in Alzheimer's disease correspond to dissociable functional brain networks. *Human Brain Mapping*, *37*, 35–53.

Habas, C., Kamdar, N., Nguyen, D., Prater, K., Beckmann, C. F., Menon, V., & Greicius, M. D. (2009). Distinct cerebellar contributions to intrinsic connectivity networks. *The Journal of Neuroscience*, *29*, 8586–8594.

Jacobs, H. I., Radua, J., Luckmann, H. C., & Sack, A. T. (2013). Meta-analysis of functional network alterations in Alzheimer's disease: Toward a network biomarker. *Neuroscience and Biobehavioral Reviews*, *37*, 753–765.

Li, H. J., Hou, X. H., Liu, H. H., Yue, C. L., He, Y., & Zuo, X. N. (2015). Toward systems neuroscience in mild cognitive impairment and Alzheimer's disease: A meta-analysis of 75 fMRI studies. *Human Brain Mapping*, *36*, 1217–1232.

Li, J., Jin, D., Li, A., Liu, B., Song, C., Wang, P., … Han, Y. (2019). ASAF: Altered spontaneous activity fingerprinting in Alzheimer's disease based on multisite fMRI. *Science Bulletin*, *64*, 998–1010.

Li, T., Wang, Q., Zhang, J., Rolls, E. T., Yang, W., Palaniyappan, L., … Feng, J. (2017). Brain-wide analysis of functional connectivity in first-episode and chronic stages of schizophrenia. *Schizophrenia Bulletin*, *43*, 436–448.

Lian, C., Liu, M., Zhang, J., & Shen, D. (2020). Hierarchical fully convolutional network for joint atrophy localization and Alzheimer's Disease diagnosis using structural MRI. *IEEE Transactions on Pattern Analysis and Machine Intelligence*, *42*, 880–893.

Liang, P., Li, Z., Deshpande, G., Wang, Z., Hu, X., & Li, K. (2014). Altered causal connectivity of resting state brain networks in amnesic MCI. *PLoS One*, *9*, e88476.

Liu, J., Zhang, X., Yu, C., Duan, Y., Zhuo, J., Cui, Y., … Liu, Y. (2016). Impaired Parahippocampus connectivity in mild cognitive impairment and Alzheimer's Disease. *Journal of Alzheimer's Disease*, *49*, 1051–1064.

Liu, M., Zhang, J., Adeli, E., & Shen, D. (2018). Landmark-based deep multi-instance learning for brain disease diagnosis. *Medical Image Analysis*, *43*, 157–168.

Liu, Y., Yu, C., Zhang, X., Liu, J., Duan, Y., Alexander-Bloch, A. F., … Bullmore, E. (2014). Impaired long distance functional connectivity and weighted network architecture in Alzheimer's disease. *Cerebral Cortex*, *24*, 1422–1435.

Liu, Z., Zhang, Y., Bai, L., Yan, H., Dai, R., Zhong, C., … Tian, J. (2012). Investigation of the effective connectivity of resting state networks in Alzheimer's disease: A functional MRI study combining independent components analysis and multivariate granger causality analysis. *NMR in Biomedicine*, *25*, 1311–1320.

MacDonald, A. W., 3rd, Cohen, J. D., Stenger, V. A., & Carter, C. S. (2000). Dissociating the role of the dorsolateral prefrontal and anterior cingulate cortex in cognitive control. *Science*, *288*, 1835–1838.

Marshall, G. A., Monserratt, L., Harwood, D., Mandelkern, M., Cummings, J. L., & Sultzer, D. L. (2007). Positron emission tomography metabolic correlates of apathy in Alzheimer disease. *Archives of Neurology*, *64*, 1015–1020.

Mega, M. S., & Cummings, J. L. (1997). The cingulate and cingulate syndromes.

Nunes, A., Schnack, H. G., Ching, C. R. K., Agartz, I., Akudjedu, T. N., Alda, M., … Group, E.B.D.W. (in press). Using structural MRI to identify bipolar disorders - 13 site machine learning study in 3020 individuals from the ENIGMA bipolar disorders working group. *Molecular Psychiatry*. https://doi.org/10.1038/s41380-018-0228-9

Pan, P., Zhu, L., Yu, T., Shi, H., Zhang, B., Qin, R., … Xu, Y. (2017). Aberrant spontaneous low-frequency brain activity in amnestic mild cognitive impairment: A meta-analysis of resting-state fMRI studies. *Ageing Research Reviews*, *35*, 12–21.

Paus, T. (2001). Primate anterior cingulate cortex: Where motor control, drive and cognition interface. *Nature Reviews. Neuroscience*, *2*, 417–424.

Postuma, R. B., & Dagher, A. (2006). Basal ganglia functional connectivity based on a meta-analysis of 126 positron emission tomography and functional magnetic resonance imaging publications. *Cerebral Cortex*, *16*, 1508–1521.

Qi, Z., Wu, X., Wang, Z., Zhang, N., Dong, H., Yao, L., & Li, K. (2010). Impairment and compensation coexist in amnestic MCI default mode network. *NeuroImage*, *50*, 48–55.

Raichle, M. E., MacLeod, A. M., Snyder, A. Z., Powers, W. J., Gusnard, D. A., & Shulman, G. L. (2001). A default mode of brain function. *Proceedings of the National Academy of Sciences of the United States of America*, *98*, 676–682.

Rathore, S., Habes, M., Iftikhar, M. A., Shacklett, A., & Davatzikos, C. (2017). A review on neuroimaging-based classification studies and associated feature extraction methods for Alzheimer's disease and its prodromal stages. *NeuroImage*, *155*, 530–548.

Richiardi, J., Altmann, A., Milazzo, A. C., Chang, C., Chakravarty, M. M., Banaschewski, T., … IMAGEN Consortium. (2015). Correlated gene expression supports synchronous activity in brain networks. *Science*, *348*, 1241–1244.

Rozycki, M., Satterthwaite, T. D., Koutsouleris, N., Erus, G., Doshi, J., Wolf, D. H., … Davatzikos, C. (2018). Multisite machine learning analysis provides a robust structural imaging signature of schizophrenia detectable across diverse patient populations and within individuals. *Schizophrenia Bulletin*, *44*, 1035–1044.

Sanz-Arigita, E. J., Schoonheim, M. M., Damoiseaux, J. S., Rombouts, S. A., Maris, E., Barkhof, F., … Stam, C. J. (2010). Loss of 'small-world' networks in Alzheimer's disease: Graph analysis of FMRI resting-state functional connectivity. *PLoS One*, *5*, e13788.

Scheltens, P., Blennow, K., Breteler, M. M. B., de Strooper, B., Frisoni, G. B., Salloway, S., & Van der Flier, W. M. (2016). Alzheimer's disease. *The Lancet*, *388*, 505–517.

Schouten, T. M., Koini, M., de Vos, F., Seiler, S., van der Grond, J., Lechner, A., … Rombouts, S. (2016). Combining anatomical, diffusion, and resting state functional magnetic resonance imaging for individual classification of mild and moderate Alzheimer's disease. *NeuroImage: Clinical*, *11*, 46–51.

Seguin, C., Razi, A., & Zalesky, A. (2019). Inferring neural signalling directionality from undirected structural connectomes. *Nature Communications*, *10*, 4289.

Sepulcre, J., Liu, H., Talukdar, T., Martincorena, I., Yeo, B. T., & Buckner, R. L. (2010). The organization of local and distant functional connectivity in the human brain. *PLoS Computational Biology*, *6*, e1000808.

Skatun, K. C., Kaufmann, T., Doan, N. T., Alnaes, D., Cordova-Palomera, A., Jonsson, E. G., … Westlye, L. T. (2017). Consistent functional connectivity alterations in schizophrenia Spectrum disorder: A multisite study. *Schizophrenia Bulletin*, *43*, 914–924.

Stonnington, C. M., Chu, C., Kloppel, S., Jack, C. R., Jr., Ashburner, J., Frackowiak, R. S., & Alzheimer Disease Neuroimaging, I. (2010). Predicting clinical scores from magnetic resonance scans in Alzheimer's disease. *NeuroImage*, *51*, 1405–1413.

Teipel, S. J., Wohlert, A., Metzger, C., Grimmer, T., Sorg, C., Ewers, M., … Dyrba, M. (2017). Multicenter stability of resting state fMRI in the detection of Alzheimer's disease and amnestic MCI. *NeuroImage: Clinical*, *14*, 183–194.

Varoquaux, G. (2018). Cross-validation failure: Small sample sizes lead to large error bars. *NeuroImage*, *180*, 68–77.

Wang, J., Zuo, X., Dai, Z., Xia, M., Zhao, Z., Zhao, X., … He, Y. (2013). Disrupted functional brain connectome in individuals at risk for Alzheimer's disease. *Biological Psychiatry*, *73*, 472–481.

Wang, K., Liang, M., Wang, L., Tian, L., Zhang, X., Li, K., & Jiang, T. (2007). Altered functional connectivity in early Alzheimer's disease: A resting-state fMRI study. *Human Brain Mapping*, *28*, 967–978.

Xia, M., Si, T., Sun, X., Ma, Q., Liu, B., Wang, L., … D.I.-M.D.D.W. Group. (2019). Reproducibility of functional brain alterations in major depressive disorder: Evidence from a multisite resting-state functional MRI study with 1,434 individuals. *NeuroImage*, *189*, 700–714.

Xu, K., Liu, Y., Zhan, Y., Ren, J., & Jiang, T. (2018). BRANT: A versatile and extendable resting-state fMRI toolkit. *Frontiers in Neuroinformatics*, *12*, 52.

Yu, M., Linn, K. A., Cook, P. A., Phillips, M. L., McInnis, M., Fava, M., … Sheline, Y. I. (2018). Statistical harmonization corrects site effects in functional connectivity measurements from multi-site fMRI data. *Human Brain Mapping*, *39*, 4213–4227.

Zang, Y., Jiang, T., Lu, Y., He, Y., & Tian, L. (2004). Regional homogeneity approach to fMRI data analysis. *NeuroImage*, *22*, 394–400.

Zaykin, D. V. (2011). Optimally weighted Z-test is a powerful method for combining probabilities in meta-analysis. *Journal of Evolutionary Biology*, *24*, 1836–1841.

Zhan, Y. F., Yao, H. X., Wang, P., Zhou, B., Zhang, Z. Q., Guo, Y. E., … Liu, Y. (2016). Network-based statistic show aberrant functional connectivity in Alzheimer's Disease. *IEEE Journal of Selected Topics in Signal Processing*, *10*, 1182–1188.

Zhang, J., Cheng, W., Liu, Z., Zhang, K., Lei, X., Yao, Y., … Feng, J. (2016). Neural, electrophysiological and anatomical basis of brain-network variability and its characteristic changes in mental disorders. *Brain*, *139*, 2307–2321.

Zhao, K., Ding, Y., Han, Y., Fan, Y., Alexander-Bloch, A. F., Han, T., … Liu, Y. (in press). Independent and reproducible hippocampal radiomic biomarkers for multisite Alzheimer's disease: Diagnosis, longitudinal progress and biological basis. *Science Bulletin*. https://doi.org/10.1016/j.scib.2020.04.003

Zhou, B., Yao, H., Wang, P., Zhang, Z., Zhan, Y., Ma, J., … Zhang, X. (2015). Aberrant functional connectivity architecture in Alzheimer's Disease and mild cognitive impairment: A whole-brain, data-driven analysis. *BioMed Research International*, *2015*, 495375.

Zhou, H. H., Singh, V., Johnson, S. C., Wahba, G., & Alzheimer's Disease Neuroimaging, I. (2018). Statistical tests and identifiability conditions for pooling and analyzing multisite datasets. *Proceedings of the National Academy of Sciences of the United States of America*, *115*, 1481–1486.

Zou, H., & Hastie, T. (2005). Regularization and variable selection via the elastic net. *Journal of the Royal Statistical Society: Series B (Statistical Methodology)*, *67*, 301–320.

SUPPORTING INFORMATION

Additional supporting information may be found online in the Supporting Information section at the end of this article.

How to cite this article: Jin D, Wang P, Zalesky A, et al. Grab-AD: Generalizability and reproducibility of altered brain activity and diagnostic classification in Alzheimer's Disease. *Hum Brain Mapp*. 2020;41:3379–3391. https://doi.org/10.1002/hbm.25023